



This paper is a part of the hereunder thematic dossier published in OGST Journal, Vol. 69, No. 6, pp. 977-1129 and available online [here](#)

Cet article fait partie du dossier thématique ci-dessous publié dans la revue OGST, Vol. 69, n°6, pp. 977-1129 et téléchargeable [ici](#)

DOSSIER Edited by/Sous la direction de : **P.-L. Carrette**

PART 2

Post Combustion CO₂ Capture Captage de CO₂ en postcombustion

Oil & Gas Science and Technology – Rev. IFP Energies nouvelles, Vol. 69 (2014), No. 6, pp. 977-1129

Copyright © 2014, IFP Energies nouvelles

- 977 > Editorial
- 989 > *Post-Combustion CO₂ Capture by Vacuum Swing Adsorption Using Zeolites – a Feasibility Study*
Captage du CO₂ en postcombustion par adsorption modulée en pression avec désorption sous vide sur zéolithes — étude de faisabilité
G. D. Pirngruber, V. Carlier and D. Leinekugel-le-Cocq
- 1005 > *Membrane Separation Processes for Post-Combustion Carbon Dioxide Capture: State of the Art and Critical Overview*
Procédés membranaires pour le captage du dioxyde de carbone : état de l'art et revue critique
B. Belaisaoui and É. Favre
- 1021 > *Pressure Drop, Capacity and Mass Transfer Area Requirements for Post-Combustion Carbon Capture by Solvents*
Pertes de charge, capacité et aires de transfert de matière requises pour le captage du CO₂ en postcombustion par solvants
A. Lassauce, P. Alix, L. Raynal, A. Royon-Lebeaud and Y. Haroun
- 1035 > *Hollow Fiber Membrane Contactors for Post-Combustion CO₂ Capture: A Scale-Up Study from Laboratory to Pilot Plant*
Captage postcombustion du CO₂ par des contacteurs membranaires de fibres creuses : de l'échelle laboratoire à l'échelle pilote industriel
É. Chabanon, E. Kimball, É. Favre, O. Lorain, E. Goetheer, D. Ferre, A. Gomez and P. Broutin
- 1047 > *Hollow Fiber Membrane Contactors for CO₂ Capture: Modeling and Up-Scaling to CO₂ Capture for an 800 MW_e Coal Power Station*
Contacteurs à membrane à fibres creuses pour la capture de CO₂ : modélisation et mise à l'échelle de la capture du CO₂ d'une centrale électrique au charbon de 800 MW_e
E. Kimball, A. Al-Azki, A. Gomez, E. Goetheer, N. Booth, D. Adams and D. Ferre
- 1059 > *Regeneration of Alkanolamine Solutions in Membrane Contactor Based on Novel Polynorbornene*
Régénération de solutions d'alcanolamine dans un contacteur à membrane basé sur un nouveau polynorbornène
A.A. Shutova, A.N. Trusov, M.V. Bermeshev, S.A. Legkov, M.L. Gringolts, E.Sh. Finkelstein, G.N. Bondarenko and A.V. Volkov
- 1069 > *Development of HiCapt+™ Process for CO₂ Capture from Lab to Industrial Pilot Plant*
Développement du procédé HiCapt+™ pour le captage du CO₂ : du laboratoire au pilote industriel
É. Lemaire, P. A. Bouillon and K. Lettat
- 1081 > *A Technical and Economical Evaluation of CO₂ Capture from Fluidized Catalytic Cracking (FCC) Flue Gas*
Évaluation technico-économique du captage du CO₂ présent dans les fumées d'une unité FCC (*Fluidized Catalytic Cracking*)
R. Digne, F. Feugnet and A. Gomez
- 1091 > *Pilot Plant Studies for CO₂ Capture from Waste Incinerator Flue Gas Using MEA Based Solvent*
Étude du captage du CO₂ dans des gaz de combustion d'un incinérateur de déchets à l'aide d'un pilote utilisant un solvant à base de MEA
I. Aouini, A. Ledoux, L. Estel and S. Mary
- 1105 > *Amine Solvent Regeneration for CO₂ Capture Using Geothermal Energy with Advanced Stripper Configurations*
Régénération d'un solvant de captage du CO₂ utilisant l'énergie géothermique et des configurations améliorées pour le régénérateur
D.H. Van Wagener, A. Gupta, G.T. Rochelle and S.L. Bryant
- 1121 > *ACACIA Project – Development of a Post-Combustion CO₂ capture process. Case of the DMX™ process*
Projet ACACIA – Développement d'un procédé de captage du CO₂ postcombustion – Cas du procédé DMX™
A. Gomez, P. Briot, L. Raynal, P. Broutin, M. Gimenez, M. Soazic, P. Cessat and S. Saisset

Amine Solvent Regeneration for CO₂ Capture Using Geothermal Energy with Advanced Stripper Configurations

D.H. Van Wagener¹, A. Gupta², G.T. Rochelle^{1*} and S.L. Bryant²

¹ Department of Chemical Engineering – C0400, The University of Texas at Austin, Austin, TX 78712 - USA

² Department of Petroleum and Geochemical Engineering – C0304, The University of Texas at Austin, Austin, TX 78712 - USA
e-mail: dvanwage@utexas.edu - abhishek.k.gupta@mail.utexas.edu - gtr@che.utexas.edu - steven_bryant@mail.utexas.edu

* Corresponding author

Résumé — Régénération d'un solvant de captage du CO₂ utilisant l'énergie géothermique et des configurations améliorées pour le régénérateur — Le captage du CO₂ dans les fumées des centrales électriques au charbon utilisant des alcanolamines nécessite un apport d'énergie substantiel. Les designs typiques prévoient l'utilisation de vapeur de pression faible à intermédiaire prélevée sur les turbines pour fournir la chaleur au rebouilleur. L'énergie géothermique issue de saumures chaudes offre une alternative à cette perte importante dans le cycle de génération d'électricité. Nous avons évalué les besoins (nombre et espacement des puits d'extraction et d'injection) pour produire de la chaleur à 150 °C à l'échelle pilote (60 MW_e) et pour une unité de taille réelle (900 MW_e) pendant trente ans. Les calculs sont basés sur les propriétés d'un aquifère géopressurisé/géothermique situé près de la côte du Golf du Texas. Cet aquifère est situé entre 3 050 et 3 350 m (10 000 et 11 000 pieds) de la surface à proximité d'une importante centrale électrique au charbon. Nous présentons un nouveau design pour le régénérateur du procédé basé sur un échange de chaleur avec la saumure, délivrant une saumure à 100 °C. Les résultats montrent que le procédé complet est faisable et que les coûts sont du même ordre de grandeur que pour le design standard.

Abstract — Amine Solvent Regeneration for CO₂ Capture Using Geothermal Energy with Advanced Stripper Configurations — Absorption/stripping using alkanolamine solvents for removing CO₂ from the flue gas of coal-fired power plants requires a substantial amount of energy. Typical designs anticipate the use of steam extraction between the Intermediate Pressure (IP) and Low Pressure (LP) turbines to provide heat for the reboiler. Geothermal energy in the form of hot brine offers an alternative to this large parasitic load on the power generation cycle. We investigate the requirements (number and spacing of extraction/injection well pairs) to provide heat at 150°C for a pilot scale (60 MW_e) and a full scale (900 MW_e) capture process for thirty years. The calculations are based on properties of a geopressured/geothermal aquifer near the Texas Gulf Coast. In the vicinity of a large coal-fired power plant in South Texas, this aquifer lies between 3 050 and 3 350 m (10 000 and 11 000 ft) below the surface. We present a novel design of the stripper/regenerator process based on heat exchange with the brine, discharging the brine at 100°C. The results indicate that the overall process is feasible and that costs are of similar magnitude to standard designs.

NOMENCLATURE

A	Well drainage area (m^2)
$C_{p, \text{brine}}$	Volumetric heat capacity of brine (J/g/K)
D	Well spacing between injector and producer of an isolated doublet (cm)
E_T	Thermal power generated (J/s)
H	Reservoir thickness (cm)
h	Water level drawdown (m)
h_t	Threshold water level drawdown for the specific formation (m)
K_R	Thermal conductivity of cap rock and bed rock ($\text{cal/cm/s/}^\circ\text{C}$)
m_{brine}	Mass flow rate of brine (g/s)
P_{in}	Pressure of overhead vapor entering compressor (bar)
Q	Constant production rate (m^3/s)
Q_i	Heat duty in reboiler/cross exchanger (kJ/mol CO_2)
Q_{max}	Maximum production rate for the specific pressure drawdown (m^3/s)
Q_s	Brine recycling rate at surface condition (cm^3/s)
r_e	Aquifer drainage radius (m)
r_w	Wellbore radius (m)
S	Aquifer storage coefficient
$T_{\text{brine, in}}$	Temperature of incoming brine to stripper (K)
$T_{\text{brine, out}}$	Temperature outlet brine from stripper (K)
T_i	Temperature of reboiler (K)
$T_{i, f}$	Exiting temperature of brine from heat exchanger (K)
$T_{i, o}$	Entering temperature of brine from heat exchanger (K)
T_{inj}	Surface temperature of injecting brine (K)
T_{prod}	Surface temperature of producing brine (K)
T_r	Aquifer transmissivity (m^2/s)
T_{sink}	Sink temperature for turbine calculations 313 K
W_{comp}	Compression work (kJ/mol CO_2)
W_{eq}	Equivalent work (kJ/mol CO_2)
W_{heat}	Electric penalty from heat usage (kJ/mol CO_2)
W_{pump}	Pump work (kJ/mol CO_2)
Δt	Time (s)
$\rho_R C_R$	Volumetric heat capacity of reservoir ($\text{cal/cm}^3/^\circ\text{C}$)
$\rho_w C_w$	Volumetric heat capacity of formation brine ($\text{cal/cm}^3/^\circ\text{C}$)
ϕ	Reservoir average porosity (fraction)

INTRODUCTION

Absorption/stripping using alkanolamine solvents is the state-of-the-art technology for removing CO_2 from the flue gas of coal-fired power plants (Rochelle, 2009). Lean solvent fed to the top of the absorber column counter-currently contacts the flue gas to absorb the CO_2 by chemical reaction. A typical coal-fired power plant emits flue gas with 12% CO_2 and the absorber captures 90% to leave 1.3%. The rich solvent is heated in a cross exchanger and then fed to the stripper. Heat applied to the rich solvent reverses the reaction and liberates the CO_2 to regenerate the lean solvent. The gaseous CO_2 is compressed for sequestration and the lean amine solvent is recycled to the absorber. The base case absorption/stripping flowsheet using 7 m Monoethanolamine (MEA) with a simple stripper column has been estimated to reduce the output of a coal-fired power plant by 25 to 30% due to the energy requirement of the reboiler, pumps and multi-stage compressor (Van Wagener, 2011). The pumps and multi-stage compressor would directly draw generated electricity but the reboiler would reroute steam from between the Intermediate Pressure (IP) and Low Pressure (LP) turbines to provide heat.

Because this re-routed steam accounts for much of the power plant output penalty, a heat source such as geothermal energy is potentially attractive alternative. The heat in the Earth's interior originated from its consolidation from dust and gases over 4 billion years ago and is continually regenerated from the decay of radioactive elements that occur in the rock. High temperature geothermal reservoirs can be utilized to generate electricity from hot water/steam. Moderate to low temperature reservoirs are generally best suited for direct use in space heating/cooling and industrial or agricultural processes. A number of geopressured/geothermal reservoirs are present along the Texas Gulf coast which can produce hot brine (150°C) at rates high enough to operate the reboiler in a CO_2 stripper. However, using geothermal brine would be very different from using steam in several respects. The heat supplied from the brine will arrive at different temperatures, depending on the reservoir, and over time, the brine produced from the same reservoir will cool if re-injected brine makes its way to the extraction wells. A typical steam reboiler would not make efficient use of geothermal brine because there would be a large approach temperature on the hot side of the exchanger and a pinch on the cold side. Alternatively, using a cross exchanger with the hot brine and cool rich solvent could more effectively take advantage of the high

temperature brine by balancing the temperature approach throughout the exchanger.

Recent work has investigated the use of multi-stage flash flowsheets to strip CO₂ as opposed to the typical simple stripper column. An isothermal 2-stage flash in place of the stripper column was demonstrated to be beneficial (Van Wagener and Rochelle, 2010). The heat supplied for the previous multi-stage flash configurations was delivered in a reboiler with steam. A form of the multi-stage flash configuration is proposed here that incorporates cool rich solvent cross exchangers to heat the solvent with brine with flashing at two different pressures.

1 STRIPPER MODELS

Concentrated aqueous piperazine (8 m PZ) was selected as the primary solvent for this study. It is thermally stable to at least 150°C. Monoethanolamine (MEA) is less useful with geothermal heat because it degrades above 120°C. As discussed in Section 3, brine is available at approximately 150°C. At a concentration of 8 m, PZ has twice the CO₂ carrying capacity of 7 m MEA, which improves the energy performance of PZ compared to MEA (Freeman et al., 2010). 5deMayo is an available thermodynamic model for aqueous PZ in Aspen Plus® (Van Wagener, 2011). This model was regressed in the electrolyte nonrandom two liquid (e-NRTL) framework to represent CO₂ solubility (Ermatchkov et al., 2006; Hilliard, 2008; Dugas, 2009; Xu and Rochelle, 2011), heat capacity, and amine volatility (Nguyen et al., 2011).

8 m PZ was simulated in an advanced 2-stage, 2-pressure flash (2T2PFlash) (Fig. 1). The configuration utilized an arrangement of five heat exchangers to remove heat from brine and the returning lean solvent. The heating in this configuration was different from traditional arrangements in that the rich solvent was fully

heated before entering the two adiabatic flash vessels in series. The first flash had the higher temperature and pressure, and the second flash dropped in both temperature and pressure.

All unit operations were modeled with chemical equilibrium within and between the gas and liquid phases. Several conditions were specified to be constant while others were optimized. A constant rich loading of 0.4 mol CO₂/mol alkalinity was specified. The input temperature of the rich solvent coming from the absorber was specified to be a constant 50°C. The lean solvent would be fed to the absorber at 40°C and a rise in solvent temperature of 10°C can be expected due to the exothermic heat of absorption. The Log Mean Temperature Difference (LMTD) was 5°C for all exchangers and a minimum approach of 1°C was specified for either side. In the base case the brine was supplied at 150°C but in all cases the return temperature for the brine was set to be 50°C cooler than the supply temperature. The temperature difference between flash vessels was varied to ensure that equal moles of vapor were generated in each flash. This specification was made to improve the reversibility of the process.

The work required for the multi-stage compressor was calculated using a correlation derived from a separate Aspen Plus® simulation (Eq. 1). The work calculation assumed a pre-condenser and intercoolers cooling to 40°C with water knockout. The number of compression stages was set to the minimum required to keep a compression ratio between stages less than 2. The final compressed CO₂ pressure was 150 bar. The split of solvent between exchangers 2 and 3 was set to 80% toward exchanger 3.

$$W_{comp} \left(\frac{\text{kJ}}{\text{mol CO}_2} \right) = \begin{cases} 4.572 \ln(150P_{in}) - 4.096, & P_{in} \leq 4.56 \text{ bar} \\ 4.023 \ln(150P_{in}) - 2.181, & P_{in} > 4.56 \text{ bar} \end{cases} \quad (1)$$

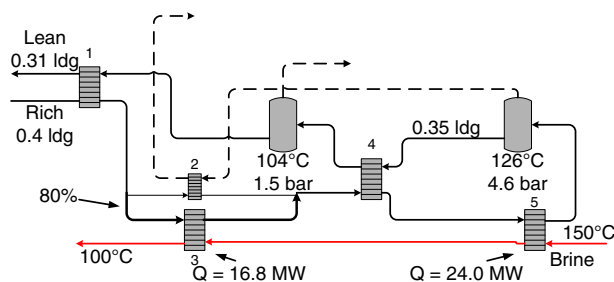


Figure 1

Advanced 2-Stage, 2-Pressure Flash (2T2Pflash) for amine solvent regeneration with geothermal brine heating.

The temperature of the first flash vessel was allowed to float to match the desired outlet brine temperature. The lean loading was manipulated by varying the brine flow rate. The overall work requirement for the pumps, multi-stage compressor, and heat duty was determined using an equivalent work expression, which calculated the total electricity usage normalized by the CO₂ removal rate (Eq. 2). The work requirement of the heat duty was calculated by Equation (3). This has been used in previous work to calculate the amount of electricity that would be generated by the power plant turbines if the steam had not been used to heat the reboilers.

This equation required the temperature of the steam, T_i . For this work, Equation (3) was integrated between the inlet and outlet temperatures to account for the changing value of heat at different temperatures, assuming that each unit of heat flow resulted in the same change in temperature along the entire temperature range. The inlet and outlet temperatures in each heater i were $T_{i,o}$ and $T_{i,f}$, respectively. This integration gave Equation (4).

$$W_{eq} = W_{heat} + W_{pump} + W_{comp} \quad (2)$$

$$W_{heat} = \sum_{i=1}^{n_{heaters}} 0.75Q_i \left(\frac{T_i + 5K - T_{sink}}{T_i + 5K} \right) \quad (3)$$

$$W_{heat} = \sum_{i=1}^{n_{heaters}} 0.75Q_i \left(\frac{T_{i,f} - T_{i,o} - T_{sink} \ln \left(\frac{T_{i,f}}{T_{i,o}} \right)}{T_{i,f} - T_{i,o}} \right) \quad (4)$$

For a comparison study for application at a demonstration being planned by NRG Energy (Stopek *et al.*, 2011), 9 m MEA was used in an alternative stripper configuration. MEA was represented by another e-NRTL model developed in Aspen Plus® (Hilliard, 2008). This model was developed similarly to the PZ model; model parameters were regressed to fit laboratory measurements. The configuration that was analyzed with MEA was a simple stripper with an adiabatic flash on the lean solvent (Fig. 2). This configuration has been patented by Fluor (Reddy *et al.*, 2007). The demonstration is designed for MEA, so the same solvent was selected for this modeling with geothermal heating. The brine heated a reboiler and a rich feed preheater. Unfortunately, the re-

boiler had a large hot side approach temperature since the solvent temperature was constant but this case represented a reconfiguration that adapted the Fluor configuration to use brine if it was already constructed to use steam from the power plant. The only additional process unit would be the cross exchanger to preheat the rich feed. The same constants were specified as for the 2-stage flash. The rich loading was specified to be 0.5 mol CO₂/mol alkalinity. This loading had an equilibrium partial pressure of CO₂ ($P^*_{CO_2}$) of 5 kPa at 40°C, a typical absorber temperature. The rich loading of 0.4 for PZ also had a $P^*_{CO_2}$ of 5 kPa at 40°C.

2 GEOTHERMAL ENERGY EXTRACTION

Geothermal energy can be extracted by producing hot water resident in the geothermal reservoir. The life of a geothermal reservoir depends mainly on the type of extraction method. Extraction methods for geothermal reservoirs are essentially the same as for conventional oil and gas reservoirs, except that reservoir life may be shortened because of lack of heat in addition to lack of pressure. There are mainly two development schemes considered to extract the energy from geothermal reservoirs, which we briefly review.

2.1 Production without Reinjection

The simplest development scheme to extract energy from geothermal reservoirs involves production of hot water from the geothermal reservoir with no reinjection of heat-depleted cold water back to the reservoir. In this case, the water will be produced at a constant temperature equal to the reservoir temperature minus the heat loss to surrounding earth formations from the bottom to the top of the well. The reservoir life in this development scheme depends on the volume of water present in the reservoir and the reservoir pressure. The water can be produced as long as the reservoir pressure is sufficient for the production rate to be sustained. The water production rate from the single well present in the center of a reservoir depends on the reservoir boundary conditions. Single well behavior can be approximated by simple analytical models that can be used to determine maximum production rate and reservoir life time.

2.1.1 Constant Pressure Boundary

For a uniform, homogeneous, isotropic, circular reservoir with constant pressure at the boundary, the

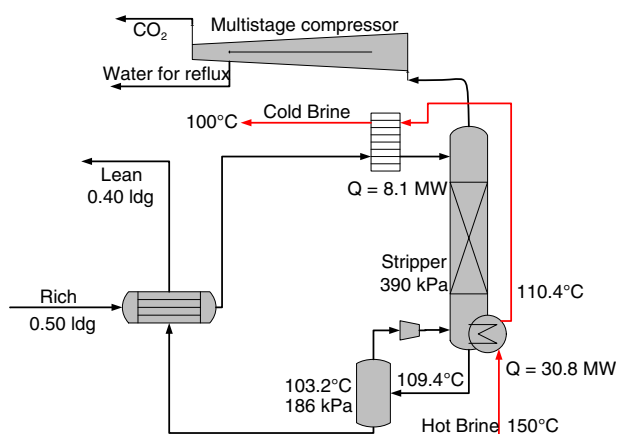


Figure 2

Fluor configuration modified for geothermal heating.

maximum pressure drawdown at the wellbore can be obtained under steady state conditions as (Dietz, 1965):

$$h = \frac{Q}{2\pi T_r} \ln \left(\frac{r_e}{r_w} \right) \quad (5)$$

Thus the maximum production rate that can be achieved for the threshold pressure drawdown is:

$$Q_{max} = \frac{2\pi T_r h_t}{\ln \left(\frac{r_e}{r_w} \right)} \quad (6)$$

2.1.2 No-Flow Boundary

For a uniform, homogeneous, isotropic, square-shaped reservoir with no-flow boundary, the maximum pressure drawdown for a well present at the center of the reservoir can be determined as (Matthews and Russell, 1967):

$$h = \frac{Q\Delta t}{SA} + \frac{Q}{4\pi T_r} \ln \left(\frac{A}{3.7r_w^2} \right) \quad (7)$$

Thus the maximum production rate that can be achieved for the threshold pressure drawdown is:

$$Q_{max} = \frac{h_t}{\frac{\Delta t}{SA} + \frac{1}{4\pi T_r} \ln \left(\frac{A}{3.7r_w^2} \right)} \quad (8)$$

2.2 Production with Reinjection

Production with reinjection involves a doublet type of development in which all produced water is reinjected into the reservoir after the heat is extracted. This helps in maintaining the reservoir pressure, and therefore in maintaining production rates, and also permits the recovery of the much larger amount of heat contained in the reservoir rock. This procedure creates a zone of injected water around the injector at a different temperature which grows with time and will eventually reach the producer. This arrival decreases temperature of produced hot water and reduces drastically the efficiency of the operation. Thus it is important to design a system of doublets with sufficient well spacing to prevent injected water breakthrough during the operation of the capture facility.

2.2.1 Single Producer and Injector Doublet

Gringarten and Sauty (1975) developed an analytical model for temperature front movement in a geothermal reservoir with single producer and injector doublet. They developed the following analytical model to determine well spacing D between injector and producer of an isolated doublet to prevent injected water breakthrough before a specified time interval Δt . See Equation (9).

2.2.2 Multi Producer and Injector Doublets

Multiple doublets are required to produce the hot water from the geothermal reservoir to meet the capture process requirements for a large power plant (> 500 MW). A study was performed by Gringarten (1977) to evaluate the effect of different doublet patterns in reservoir life and ultimate heat recovery from the reservoir. They found that the ratio of the reservoir lifetime with various two doublet patterns to that of a single doublet depends on the ratio of distance between two doublets and the well spacing between injector and producer in an individual doublet. The ratio of reservoir lifetime increases with the ratio of distance between two doublets and the well spacing between injector and producer of an individual doublet. They also performed a similar study for different multi-doublet (more than two) patterns and found that the reservoir lifetime for a multi-doublet development scenario is always less than that of single doublet in an infinite system.

3 RESERVOIR MODELING

Similar to conventional hydrocarbon reservoirs, geothermal reservoirs are complex hydrothermal systems involving single-or multi-phase fluid flow. Numerical simulation of such reservoirs is helpful in estimating the recoverable energy, in determining the optimum management techniques and improving the understanding of the reservoir geometry, and in estimating boundary conditions and rock properties. CMG-STARS (Steam, Thermal and Advanced processes Reservoir Simulator) reservoir simulator was used to model fluid and temperature front movement in a geothermal brine reservoir.

$$D = \left[\frac{2Q_s \Delta t}{\left(\varphi + (1 - \varphi) \frac{\rho_R C_R}{\rho_w C_w} \right) H + \left\{ \left(\varphi + (1 - \varphi) \frac{\rho_R C_R}{\rho_w C_w} \right)^2 H^2 + 2 \frac{K_R \rho_R C_R}{(\rho_w C_w)^2} \Delta t \right\}^{0.5}} \right]^{0.5} \quad (9)$$

4 CASE STUDY: WILCOX RESERVOIR

The Wilcox group is one of the oldest thick sand/shale sequences within the Gulf coast tertiary system. It crops out in a 16 to 32 km wide band and dips coastward into subsurface. The presence of growth faults along the shoreline of large delta lobes in the neighborhood of the Wilcox group of formations restricts the fluid flow across the growth faults (Bebout *et al.*, 1979). This caused an increase in pressure gradient at depths greater than 10 000 ft from a normal hydrostatic pressure gradient of 0.44 psi/ft to between 0.7 and 1.0 psi/ft and temperature gradient from a normal 1.8°C/100 m to

between 2.7 and 3.6°C/100 m (Bebout *et al.*, 1979). This faulted downdip section of the Wilcox group, which exhibits a large pressure gradient and temperature exceeding 149°C (300°F), comprises the Wilcox geothermal corridor as given in Figure 3. The Wilcox group of reservoirs is located beneath large coal-fired power plants in Texas where CO₂ capture is being considered. Thus geothermal fairways of the Wilcox group of reservoirs can be utilized to provide geothermal energy to capture CO₂ produced by coal-fired electric power plants.

Due to its good porosity and permeability characteristics the Dewitt fairway in the Wilcox group is used to

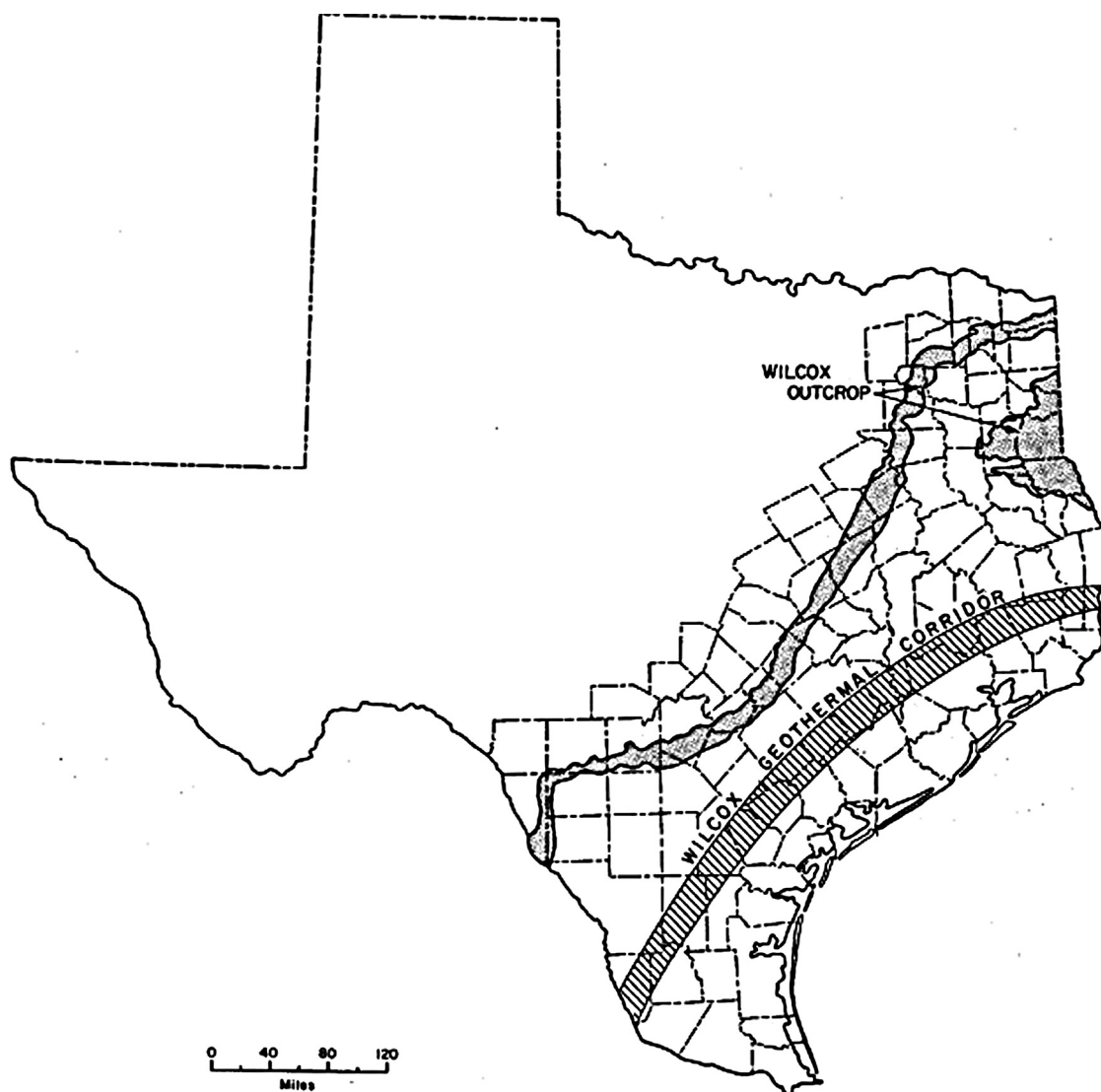


Figure 3

Texas geographical map showing the location of Wilcox outcrop and Wilcox geothermal corridor (Bebout *et al.*, 1979).

TABLE 1
Reservoir rock and brine properties used in all the reservoir simulation studies

Property	Unit	Value
Average porosity, ϕ	%	20
Average matrix permeability, k_h	mD	100
k_v/k_h	Fraction	1.0
Reservoir depth	Ft	10 500
Reservoir thickness	Ft	550
Initial reservoir temperature	°F	302
Initial reservoir pressure	Psi	4 900 @10 500 ft
Reservoir rock thermal conductivity	Btu/ft-day-°F	44
Reservoir brine thermal conductivity	Btu/ft-day-°F	8.6
Volumetric heat capacity of cap rock and bed rock	Btu/ft ³ -°F	35
Thermal conductivity of cap rock and bed rock	Btu/ft-day-°F	44
Injection water temperature	°F	208.4
Well bore tubing outside diameter	Inch	6.625
Down hole pump power for producing well	kW	1 000
Extraction period	Years	30

study the feasibility of geothermal energy extraction in this paper. At the site of the W. A. Parish plant in South Texas, the Dewitt is 10 500 ft beneath the surface. Here, we report on a strategy to generate geothermal power sufficient to drive a pilot-scale capture process for 60 MWe power generation. We then scale up 15 times to examine the well spacing requirements for a full-scale capture process for a 900 MWe coal-fired power plant.

4.1 Geothermal Modeling

A homogeneous reservoir of 640 km² (64 km × 10 km) surface area with no-flow at the reservoir boundary is used for the study. The reservoir is located 10 500 ft below the Earth surface. The whole reservoir is divided in 100 grid cells in x -direction (larger dimension) and 60 grid cells in y -direction (smaller dimension). Wells are drilled mainly in the center of the reservoir, thus fine grid sizing is used at the center with coarser grid cells towards the boundary of the reservoir. The reservoir thickness of 550 ft is divided in 11 equally sized layers. Reservoir and brine properties used in the simulation study are given in Table 1. Injection and production

wells are drilled with well spacing required to maintain constant temperature brine production at the surface.

Overburden and underburden heat gain from the cap rock and bed rock respectively is considered in all the simulations. CMG-STARS utilizes a semi-analytical model to determine heat gain due to overburden and underburden of cap rock and bed rock (Vinsome and Westerveld, 1980). The semi-analytical model calculates heat transfer rate and its derivative with respect to temperature on the basis of thermal conductivity and heat capacity of the cap and bed rock. A separate simulation study is performed to evaluate the effect of overburden and underburden heat gain on temperature front movement in the reservoir. In this simulation study, a similar set of grid cells with zero porosity is included above and below the actual reservoir to allow gradual temperature variation from cap and bed rock to the brine reservoir. The results from this simulation study indicate that the effective heat transfer coefficient in CMG-STARS approximates the more accurate solution of heat transfer from cap and bed rock to the brine reservoir. The temperature of cap rock and bed rock is considered the same as the reservoir temperature at initial conditions.

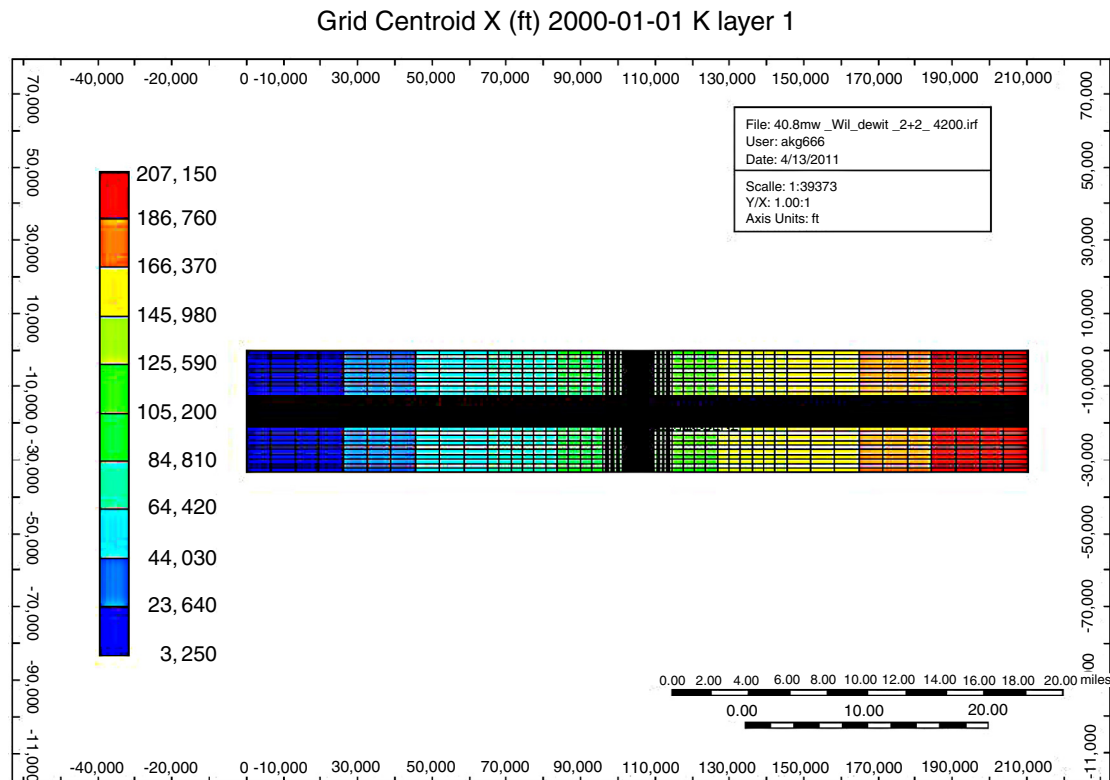


Figure 4

Topmost layer of the grid structure for pilot study showing reservoir size (64 km by 10 km). The black portion in the plot is fine grid cells with grid size of 210 ft in x and y -directions. The injection/extraction well doublets are located within the central portion of the fine grid (cf. zoomed-in view in Fig. 5). The color bar indicates the distance from the leftmost boundary of the reservoir with blue color showing reservoir portion close to left boundary and red color showing reservoir portion close to the rightmost boundary of the reservoir.

4.1.1 Pilot Study

A reservoir simulation study for a pilot power generation of 60 MW_e is performed in the CMG-STARS reservoir simulator. The target operation period is 30 years. Brine extraction/injection rate required for obtaining 41.2 MW of thermal energy for the given temperatures of produced and injected brine is determined by the simple relationship between brine mass and energy generated:

$$E_T = m_{brine} C_{p, brine} (T_{prod} - T_{inj}) \quad (10)$$

The brine rate required for the given set of conditions is 108 000 bbl/day. Two injector/producer doublets are used to achieve the required recycling rate. Each well is produced/injected at a rate of 54 000 bbl/day of brine. Two downhole pumps, each with 1 000 kW capacity, are required to pump the hot brine to the surface at the required rate. Thus a part of the extracted geothermal energy will be utilized to the run the project.

Historically, the cost of drilling and completing an onshore well such as is required for the pilot study is approximately 5 million US dollars per well, making an estimated total of 20 million US dollars for drilling and completion of the 4 wells for the pilot study. The well spacing between an injector and a producer of a doublet required to maintain the constant temperature brine production at surface for the duration of the project is determined by using the analytical model given in Equation (9). The well spacing (D) calculated using the above model for the given reservoir and fluid parameters is 130 332 cm (4 276 ft). The well spacing between two doublets is considered the same as the well spacing between the injector and producer of a doublet.

The topmost layer of the grid structure used in the simulation is given in Figure 4. The grid structure shows the reservoir size in x -direction (larger dimension). From the grid structure, it is evident that the wells are drilled at the center of the reservoir which has fine gridding at the

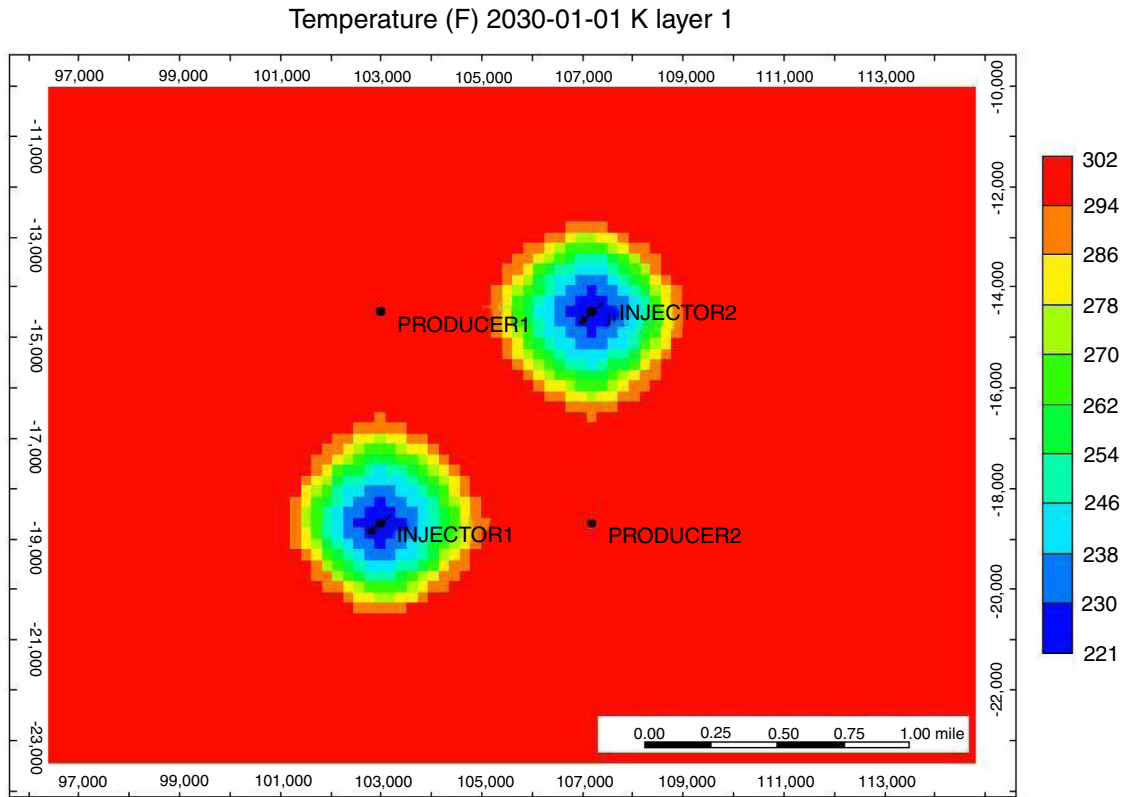


Figure 5

Topmost layer of the reservoir showing temperature front movement from injector to producer at the end of extraction period (30 years from the beginning). Wells flow at 54 000 B/D and are spaced about 4 300 ft apart. Cool regions near the injection wells show the advance of injected brine temperature; the red color corresponds to the initial reservoir temperature.

center and coarse gridding towards the boundary of the reservoir.

Figure 5 is a zoomed-in map view of the top most layer of the reservoir showing temperature front movement at the end of the extraction period (30 years from the beginning). Blue color close to injector representing low temperature values close to injection brine temperature, shows the cooling of reservoir rock due to cold brine injection. The temperature front is moving from injectors towards the producers. The red color close to producer representing high temperature value close to initial reservoir temperature shows that temperature front has not yet reached the producer.

From Figure 5, it is evident that the well separation of 4 300 ft permits constant temperature brine production for the target operating period of thirty years.

Figure 6 is the topmost layer of the reservoir showing injected brine front movement from injectors towards the producers at the end of extraction period (30 years from the beginning). The well pattern permits very

effective sweep of native formation brine from injectors to the producers. From Figures 5 and 6, it is evident that the brine front travels faster than the temperature front in the reservoir. The lag of the temperature front occurs because the reservoir rock releases heat to the cooler injected brine. A smaller contribution to the lag is the additional heat gain from the cap rock and the bed rock.

4.1.2 Scaled-Up Study

The pilot project to capture CO₂ from 60 MW_e electric power is scaled up to 900 MW_e of electric power. The geothermal power requirement scales proportionately. Thus 618 MW thermal power will be required. The number of wells is also increased by the same proportion to 30 doublets of injector and producer pairs, each having a brine recycle rate of 54 000 bbl/day. Thirty downhole pumps for each producer with 1 000 kW capacity are required to pump geothermal brine to the

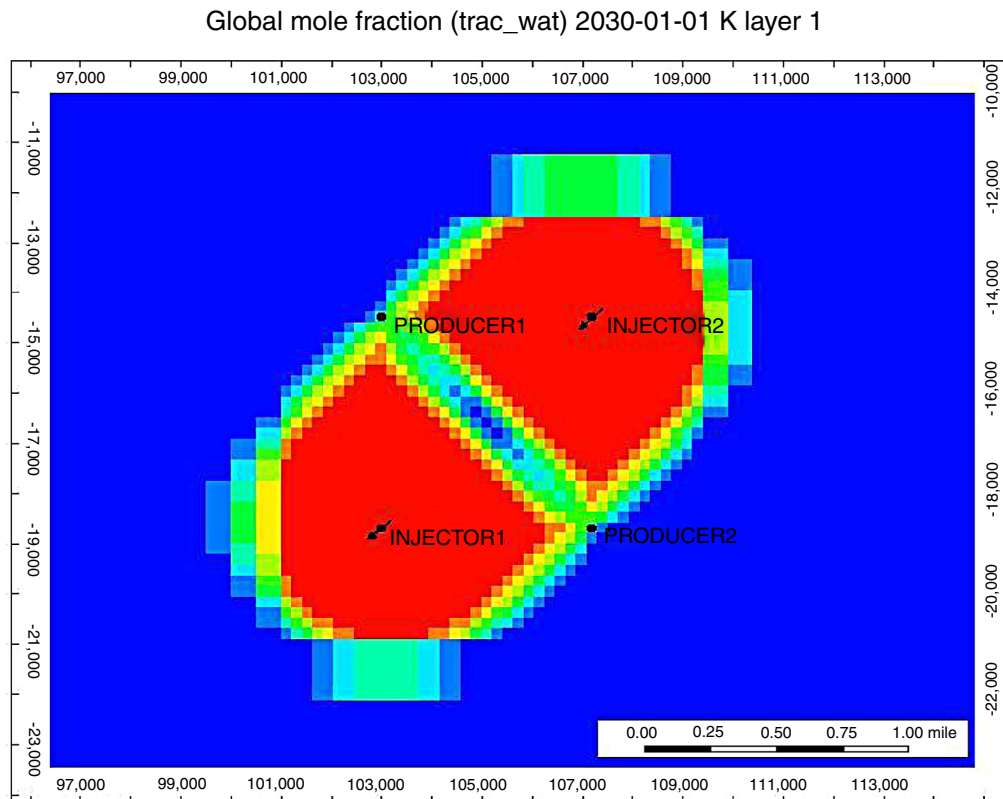


Figure 6

Same view as Figure 5 showing injection brine front movement (indicated by concentration of a tracer that moves at fluid velocity) at the end of extraction period (30 years from the beginning). Blue color shows 100% native brine mole fraction and red color shows maximum injection brine mole fraction.

surface at the required rate. Thus 30 MW_e of the total extracted geothermal power will be utilized to run down-hole pumps. The well spacing between two doublets and an injector and a producer of an individual doublet are kept constant at 4 276 ft. The total well footprint area required to extract 618 MW of thermal power for 30 years is 33 mile². In this scenario, 30 producers and 30 injectors are placed in 33 mile² area and a surface transportation system is required to transport the produced brine from well heads to the stripping plant and injection brine from stripping plant to various injectors. The topmost layer of the grid structure used in the scaled-up reservoir simulation study is shown in Figure 7.

Figure 8 is the topmost layer of the reservoir showing temperature front at the end of the extraction period (30 years from the beginning). As in Figure 5, high temperature value close to initial reservoir temperature shows that temperature front has not yet reached the producers.

Figure 9 is the topmost layer of the reservoir showing injected brine front movement from injectors towards

the producers at the end of extraction period (30 years from the beginning). From the plot it is evident that the well pattern permits the maximum sweep of native formation brine from the injectors to the producers.

4.2 Surface Utilization

The 2T2PFlash configuration was scaled to regenerate enough solvent to treat the flue gas of a 60 MW_e power plant. The flue gas from this size power plant was estimated by scaling an industrial estimate. Approximately 1 195 ton CO₂/day would be removed for 60 MW_e (Fisher *et al.*, 2005). The lean loading was optimized to minimize the overall work requirement. Relevant operating conditions for the optimized case are detailed in Figure 1.

Figure 10 shows the behavior of both equivalent work and total heat duty as a function of lean loading. The optimum equivalent work was at a lean loading of approximately 0.33 but the heat duty was minimized at

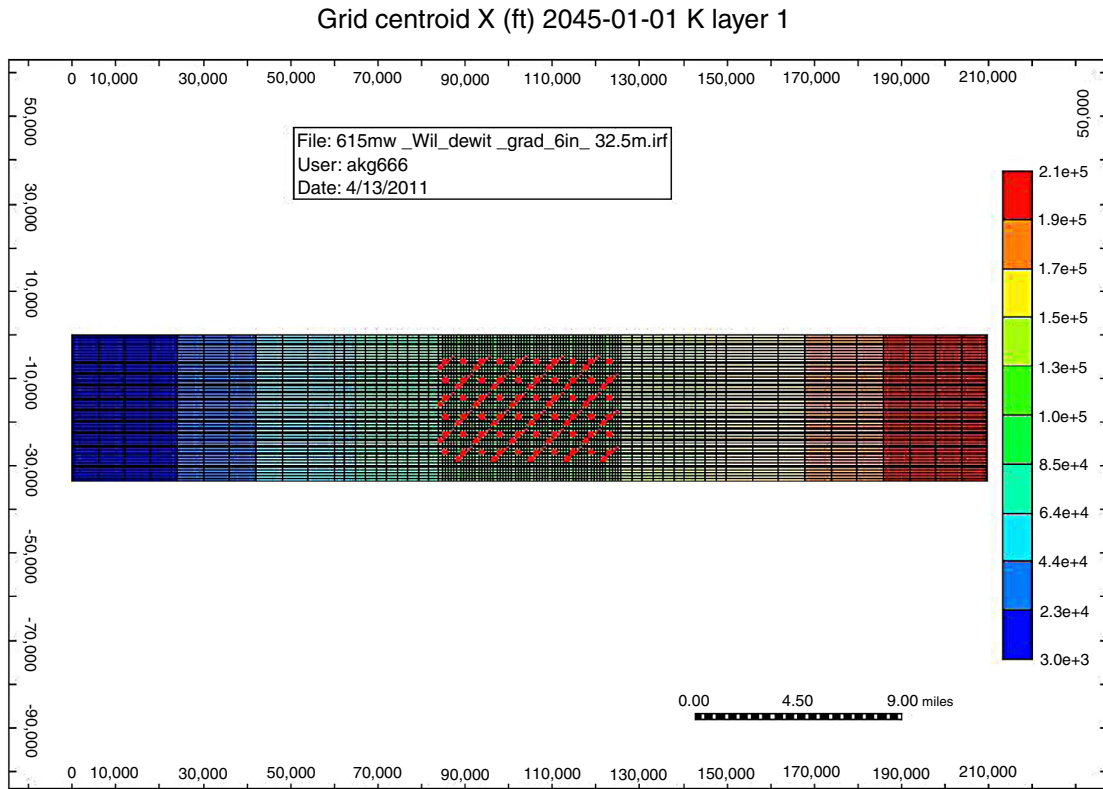


Figure 7

Topmost layer of the grid structure for scaled up study showing a 33 square mile well field of 30 injector/producer pairs in a 64 km by 10 km reservoir. Color bar as in Figure 4.

a slightly higher lean loading of 0.335. These results were calculated using a rich loading of 0.4, corresponding to a $P^*_{CO_2}$ of 5 kPa at 40°C. At the lean loading of 0.33, the equivalent work was 35.1 kJ/mole CO₂.

The $P^*_{CO_2}$ at 40°C for the optimum lean loading of 0.335 was approximately 0.85 kPa. Since the absorber would operate with 90% removal from CO₂ partial pressures of 12 kPa to 1.2 kPa, solvent concentrations representing a gas side removal of less than 90% might not provide adequate absorber performance. An overstripped lean solvent would perform well in the absorber because it would have a significant driving force to achieve the desired clean gas purity. Additionally, the lower lean loading would reduce the solvent circulation rate. Conversely, an understripped lean solvent would have trouble attaining the desired purity of 1.2% without using chilled water for cooling or excessive packing. For this reason, the operation point was chosen to have a lean loading of 0.31, where the $P^*_{CO_2}$ at 40°C was

0.5 kPa. At this lower lean loading, the equivalent work was 35.5 kJ/mole CO₂.

Since the temperature of the extracted brine was expected to decline over the length of the project, the sensitivity of the stripper performance with brine temperature was investigated. The change in temperature of the brine across the process was held constant at 50°C for all extraction temperatures. The base case temperature of 150°C required 40.8 MW of heat. The expected decrease in brine temperature over a 30-year period was 2°C. A reduction in brine temperature from 150°C to 148°C would change the heat duty to 41.2 MW, only a 2.4% increase from the design case. An extreme scenario where the brine temperature dropped to 145°C required 42.4 MW of heat, only 3.7% greater than the design case. If a brine formation that could supply heat at 160°C was found, the heat duty would decrease to 38.8 MW, a 4.5% drop from the design case. Figure 11 displays the increase in heat duty and the equivalent

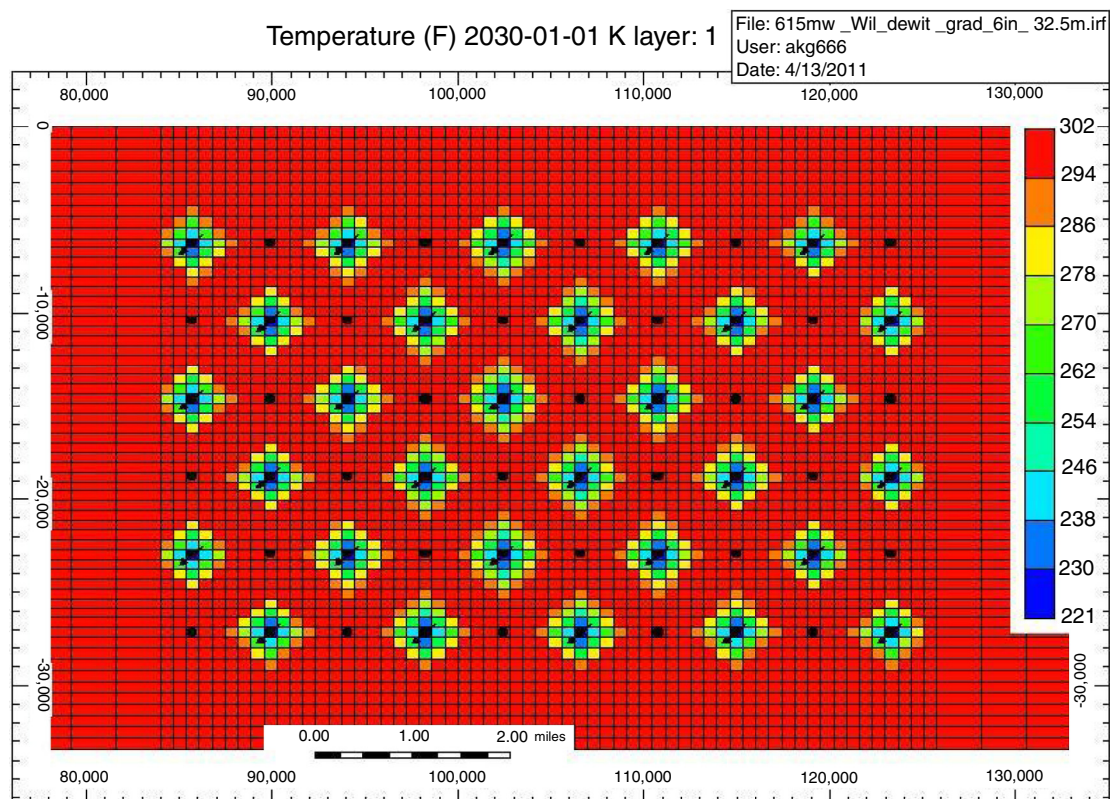


Figure 8

Topmost layer of the reservoir for 30 well pairs producing 618 MW geothermal energy shows temperature front is still far from producers at the end of extraction period (30 years from the beginning). The blue color shows low temperature close to injection brine temperature and red color shows the high temperature close to initial reservoir temperature.

work with decreasing brine temperature. Each simulation converged multiple heat exchange recycle loops at once, and the tolerance set on each recycle loop resulted in a small variability of each point. However, a general negative linear trend was observed.

The Fluor configuration was also optimized for lean loading with 9 m MEA. As has been found in previous work with MEA, the optimum lean loading was in the overstripping region (Van Wagener and Rochelle, 2010). The minimum equivalent work was 36.3 kJ/mole CO_2 at a lean loading of 0.39, seen in Figure 12. The overall heating requirement for a 60 MW plant was 38.6 MW, a lower heat duty than the 40.8 MW required in the PZ calculation. Previous work demonstrated a similar outcome, where a 2-stage flash with 8 m PZ had a higher heat duty than a simple stripper with 9 m MEA. Even though the heat duty was less for MEA, the PZ solvent made up in overall performance by operating at a higher pressure, so the 2-stage flash had a sig-

nificantly smaller compression work. Overall, 9 m MEA had a higher equivalent work requirement than 8 m PZ. These calculations with MEA used a rich loading of 0.5 with a $P^*_{\text{CO}_2}$ at 40°C of 5 kPa, and the optimum lean loading of 0.39 had a $P^*_{\text{CO}_2}$ at 40°C of 0.13 kPa. Therefore, the optimum lean loading was an acceptable range to be coupled with an absorber and expect adequate performance. Relevant operating conditions for this optimal case are detailed in Figure 12.

The difference in proportions of the three work contributions demonstrated that each configuration/solvent combination could have its own application. Using the 2T2Pflash with 8 m PZ would be advantageous when aiming to minimize the overall energy usage. However, the Fluor configuration with 9 m MEA would be advantageous if electricity was cheap and the goal was to minimize the heat usage as much as possible. The Fluor configuration with 9 m MEA reduced the heat duty from the 2-stage flash design case by 5.3%.

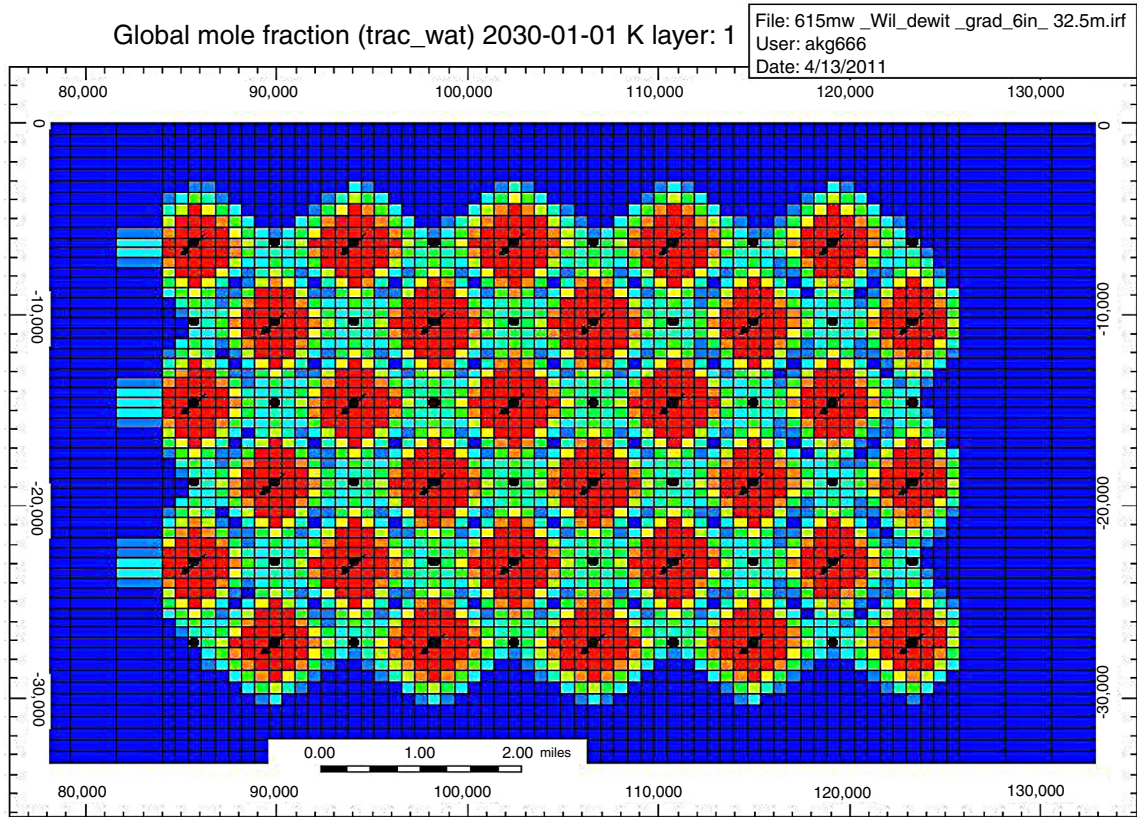


Figure 9

Topmost layer of the reservoir in scaled-up study showing injection brine front movement at the end of extraction period (30 years from the beginning). Blue color shows 100% native brine mole fraction and red color shows maximum injection brine mole fraction.

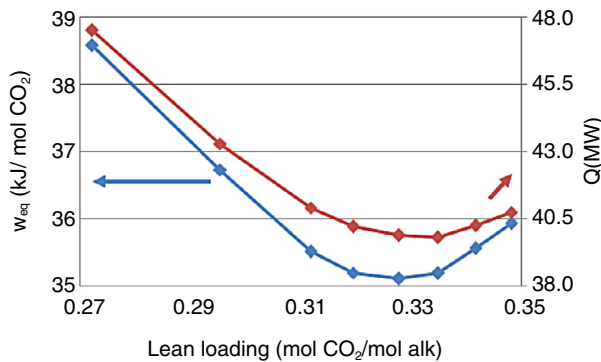


Figure 10

Lean loading optimization for 2T2Pflash with 8 m PZ. 0.40 rich loading, $T_{brine,in} = 150^{\circ}\text{C}$, $T_{brine,out} = 100^{\circ}\text{C}$, 5°C LMTD on heat exchangers, CO₂ compression to 150 bar.

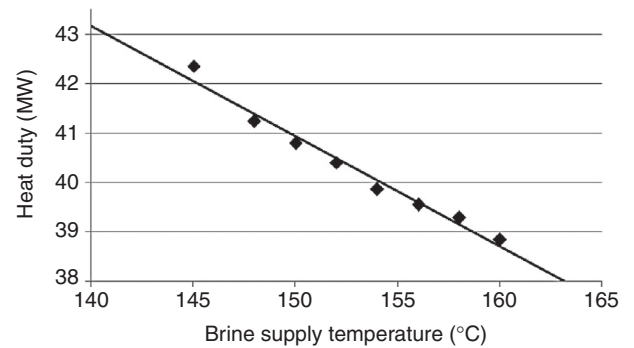


Figure 11

Reduction in total heat duty with increasing brine temperature for 2T2Pflash with 8 m PZ. 0.40 rich loading, $\Delta T_{brine} = 50^{\circ}\text{C}$, 5°C LMTD on heat exchangers, CO₂ compression to 150 bar. Points = simulation results, line = approximate linear representation.

Previous work calculated a potential minimum energy requirement for an optimized interheated stripper column with a maximum temperature of 150°C to use

30.5 kJ/mol CO₂ (Van Wagener, 2011). The best performance from this work using PZ and the 2T2P Flash configuration was 35.5 kJ/mol CO₂, an increase of 16%.

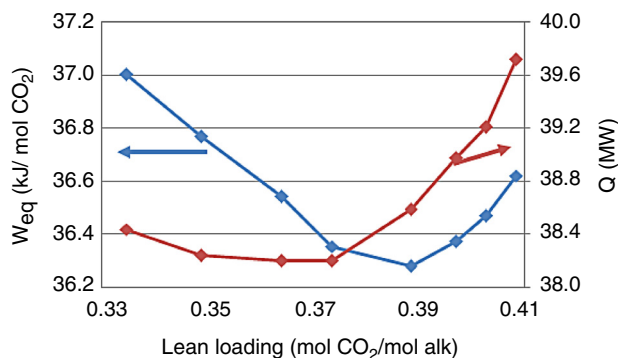


Figure 12

Lean loading optimization for Fluor configuration with 9 m MEA. 0.5 rich loading, $T_{brine,in} = 150^{\circ}\text{C}$, $T_{brine,out} = 100^{\circ}\text{C}$, CO_2 compression to 150 bar.

CONCLUSIONS

Well spacing of 4 276 ft in 30 years of operation is satisfactory to provide a constant brine temperature over the lifetime of the wells.

The reservoir simulation studies demonstrated that enough thermal energy can be extracted to regenerate the amine solvent for CO_2 capture. The reservoir models followed the proposed analytical method by Gringarten and Sauty (1975) to ensure that the simulations capture the full physics of the temperature front movement in a geothermal reservoir.

The advanced 2-stage flash with 8 m PZ demonstrated the best performance. The design case was selected to be the advanced 2-stage flash using 8 m PZ, treating flue gas generated by the production of 60 MW_e . A conservative estimate of the brine extraction temperature was 148°C , allowing for heat loss during the transportation from underground reservoir to well head along the wellbore.

Assuming a rich loading of 0.40, the heating requirement was 41.2 MW, and the overall equivalent work was 11.1 MW_e or 35.5 kJ/mol CO_2 . Of the overall equivalent work, the total contribution from heating was 6.5 MW_e or 20.6 kJ/mol CO_2 . The balance of the total work, 4.6 MW_e , was electricity directly drawn for pump work and CO_2 compression to 150 bar. This electricity would be drawn directly from the generation of the turbines, as in any proposed post-combustion carbon capture with amines. The energy requirement is 16% greater than optimized flowsheets using higher temperature steam from the coal-fired power plant. However, this flowsheet would avoid disrupting the steam cycle to draw heat for the solvent regeneration. The process

integration and control of this heating option, therefore, could be very beneficial.

In the pilot-scale study, four wells would be required to provide the geothermal heat to regenerate the solvent and save 11.1 MW_e that would otherwise be required as steam heat from the power cycle. At \$5 million/well, the estimated capital cost of saving 11.1 MW_e would be about \$1 800/kW. This is comparable to the capital cost of replacing coal-fired power capacity with new plants. The extracted thermal energy could be increased to full-scale with a similarly-scaled increase in the number of wells and land area used by wells.

ACKNOWLEDGMENTS

This work was supported by the Luminant Carbon Management Program and by the Geologic CO_2 Storage Industrial Affiliates Program at the Center for Petroleum and Geosystems Engineering, both at the University of Texas at Austin.

REFERENCES

- Bebout D.G., Weise B.R., Gregory A.R., Edwards M.B. (1979) *Wilcox sandstone reservoirs in the deep surface along the Texas Gulf coast, their potential for production of geopressed geothermal energy*, Bureau of Economic Geology, The University of Texas at Austin, October.
- Dietz D.N. (1965) Determination of average reservoir pressure from build-up surveys, *J. Petrol. Technol.* **17**, 8, 955-959, SPE-1156-PA.
- Dugas R.E. (2009) Carbon Dioxide Absorption, Desorption, and Diffusion in Aqueous Piperazine and Monoethanolamine, *PhD Thesis*, University of Texas at Austin.
- Ermachkov V., Kamps A.P.-S., Speyer D., Maurer G. (2006) Solubility of Carbon Dioxide in Aqueous Solutions of Piperazine in the Low Gas Loading Region, *J. Chem. Eng. Data* **51**, 5, 1788-1796.
- Fisher K.S., Beutkerm C., Rueter C., Searcy K. (2005) *Integrating MEA Regeneration with CO_2 Compression and Peaking to Reduce CO_2 Capture Costs*, Final DOE Report.
- Freeman S.A., Dugas R.E., Van Wagener D.H., Nguyen T., Rochelle G.T. (2010) Carbon dioxide capture with concentrated, aqueous piperazine, *Int. J. Greenhouse Gas Control* **4**, 2, 119-124.
- Gringarten A.C., Sauty J.P. (1975) A Theoretical Study of Heat Extraction from Aquifers with Uniform Regional Flow, *J. Geophys. Res.* **80**, 35, 49-56.
- Gringarten A.C. (1977) Reservoir Lifetime and Heat Recovery Factor in Geothermal Aquifers used for Urban Heating, *Pure Appl. Geophys.* **117**, 1-2, 297-308.
- Hilliard M.D. (2008) A Predictive Thermodynamic Model for an Aqueous Blend of Potassium Carbonate, Piperazine and Monoethanolamine for Carbon Dioxide Capture from Flue Gas, *PhD Thesis*, The University of Texas at Austin.

Matthews C.S., Russell D.G. (1967) Pressure buildup and flow tests in wells, SPE Monograph Series **1**, ISBN: 978-0-89520-200-0.

Nguyen T., Hilliard M.D., Rochelle G.T. (2011) Volatility of aqueous amines in CO₂ capture, *Energy Procedia* **4**, 1624-1630.

Reddy S., Gilmartin J., Francuz V. (2007) *Integrated Compressor/Stripper Configurations and Methods*, International Patent WO 2007075466.

Rochelle G.T. (2009) Amine Scrubbing for CO₂ Capture, *Science* **325**, 5948, 1652-1654.

Stopek D., Scherffius J., Klumpyan J., Smith R., Reddy S. (2011) *Carbon Capture Demonstration Project at WA Parish Station*, Electric Power 2011, Rosemont, Illinois.

Van Wagener D.H. (2011) *Stripper Modeling for CO₂ Removal Using Monoethanolamine and Piperazine Solvents*, PhD Thesis, The University of Texas at Austin.

Van Wagener D.H., Rochelle G.T. (2010) Stripper Configurations for CO₂ Capture by Aqueous Monoethanolamine, *Chem. Eng. Res. Des.* **89**, 9, 1639-1646, doi: 10.1016/j.cherd.2010.11.011.

Vinsome P.K.W., Westerveld J. (1980) A simple method for predicting cap and base rock heat losses in thermal reservoir simulators, *J. Can Petrol Technol.* **19**, 87-90.

Xu Q., Rochelle G.T. (2011) Total Pressure and CO₂ Solubility at High Temperature in Aqueous Amines, *Energy Procedia* **4**, 117-124.

Manuscript accepted in December 2012

Published online in July 2013

Copyright © 2013 IFP Energies nouvelles

Permission to make digital or hard copies of part or all of this work for personal or classroom use is granted without fee provided that copies are not made or distributed for profit or commercial advantage and that copies bear this notice and the full citation on the first page. Copyrights for components of this work owned by others than IFP Energies nouvelles must be honored. Abstracting with credit is permitted. To copy otherwise, to republish, to post on servers, or to redistribute to lists, requires prior specific permission and/or a fee: Request permission from Information Mission, IFP Energies nouvelles, fax. +33 1 47 52 70 96, or revueogst@ifpen.fr.